

Constraints on the velocity dispersion of Dark Matter from Cosmology and new bounds on scattering from the Cosmic Dawn.

IVÁN RODRÍGUEZ-MONTOYA,^{1,2} VLADIMIR ÁVILA-REESE,³ ABDEL PÉREZ-LORENZANA,⁴ AND JORGE VENZOR⁴

¹*Consejo Nacional de Ciencia y Tecnología. Av. Insurgentes Sur 1582, 03940, Ciudad de México, México*

²*Instituto Nacional de Astrofísica, Óptica y Electrónica. Apdo. Post. 51 y 216, 72000. Puebla Pue., México*

³*Instituto de Astronomía, Universidad Nacional Autónoma de México, Apdo. Post. 70-264, 04510 Ciudad de México, México*

⁴*Departamento de Física, Centro de Investigación y de Estudios Avanzados del I.P.N. Apdo. Post. 14-740, 07000, Ciudad de México, México.*

Submitted to ApJ

ABSTRACT

The observational value of the velocity dispersion, Δv , is missing in the Dark Matter (DM) puzzle. Non-zero or non-thermal DM velocities can drastically influence Large Scale Structure and the 21-cm temperature at the epoch of the Cosmic Dawn, as well as the estimation of DM physical parameters, such as the mass and the interaction couplings. To study the phenomenology of Δv we model the evolution of DM in terms of a simplistic and generic Boltzmann-like momentum distribution. Using cosmological data from the Cosmic Microwave Background, Baryonic Acoustic Oscillations, and Red Luminous Galaxies, we constrain the DM velocity dispersion for a broad range of masses $10^{-3} \text{ eV} < m_\chi < 10^9 \text{ eV}$, finding $\Delta v_0 \lesssim 0.33 \text{ km s}^{-1}$ (99% CL). Including the EDGES T_{21} -measurements, we extend our study to constrain the baryon-DM interaction in the range of DM velocities allowed by our analysis. As a consequence, we present new bounds on two electromagnetic models of DM, namely minicharged particles (MCPs) and electric dipole moment (EDM). For MCPs, the parameter region that is consistent with EDGES and independent bounds on cosmological and stellar physics is very small, pointing to the sub-eV mass regime of DM. A window in the MeV–GeV may still be compatible with these bounds for MCP models without a hidden photon. But the EDM parameter region consistent with EDGES is excluded by Big-Bang Nucleosynthesis and Collider Physics.

Keywords: cosmology: dark matter, large-scale structure of universe, dark ages, reionization, first stars; astroparticle physics, neutrinos

1. INTRODUCTION

Within the current cosmological paradigm, where Dark Matter (DM) dominates in the mass content of the Universe, the nature of the DM particles plays a key role in shaping the linear Matter Power Spectrum (MPS) and the Angular Power Spectrum of the Cosmic Microwave Background (CMB) anisotropies. Since the earliest works on the topic, the empirical evidence has favored collisionless DM particles, whose velocity dispersion in the early Universe is so small that perturbations of galaxy size or larger are not damped by free

streaming, i.e., the particles are cold (Peebles 1982; Blumenthal et al. 1984; Davis et al. 1985). The Cold DM scenario is actually fully consistent with current CMB and large-scale structure (LSS) data (see e.g., Ade et al. 2016; Aghanim et al. 2018). However, at small scales, this scenario seems to face issues, especially related to the abundance and properties of dwarf galaxies (for a recent review, see Bullock & Boylan-Kolchin 2017). Early studies based on N-body cosmological simulations have shown that these potential issues are alleviated if the DM particles are warm (Colín et al. 2000; Bode et al. 2001; Avila-Reese et al. 2001). More recent works, using semi-analytical models and N-body + Hydrodynamics cosmological simulations confirm that the Warm DM scenario for particle masses within a given range, while keeping the success of the Cold DM one at large scales,

helps to solve their potential issues at small scales (e.g., Lovell et al. 2012, 2016; Colín et al. 2015; González-Samaniego et al. 2016; Bozek et al. 2016; Bose et al. 2017, for more references, see the review by Abazajian 2017).

Thus, one of the key pieces of the DM puzzle remains up in the air, whether it is entirely cold or mildly warm. Moreover, none of the popular Cold DM candidates has been detected so far, neither directly nor indirectly. Consequently, the broad window of DM possibilities is still open for a rich variety of particles conceived in extended theories of the Standard Model. Among the most relevant and general properties of the DM particles are their rest mass m_χ and relic velocity dispersion Δv . In this sense, *it would be very useful to constrain these properties in a generic way with the CMB and LSS data.*

On the other hand, the radio signal recently detected by the Experiment to Detect the Global Epoch of Reionization Signature (EDGES, Bowman et al. 2018), not only represents the first evidence of the epochs of the Cosmic Dawn, but its anomalous absorption profile also suggests the first sign of DM non-gravitational interactions with baryons. The observed absorption trough was found too deep compared to previous theoretical notions, albeit one explanation (among others discussed below) could be that baryons were cooled down through some interaction with DM (see e.g. Dvorkin et al. 2014; Tashiro et al. 2014; Muñoz et al. 2015; Barkana 2018; Berlin et al. 2018; Safarzadeh et al. 2018). In this regard, noteworthy studies have included cosmological data such as the CMB and Lyman-alpha ($Ly-\alpha$) forest, providing valuable insights into the physics involving baryon-DM interactions, especially in the mass regime above MeV's (Chen et al. 2002; Xu et al. 2018; Slatyer & Wu 2018; Boddy & Gluscevic 2018; Boddy et al. 2018; Gluscevic & Boddy 2018; Kovetz et al. 2018). An important ingredient of this scenario that has received little attention is the DM relic velocity dispersion mainly for particles lighter than a few MeV's, even though its effects may play a major role.

In this paper, we explore limits of DM velocity dispersion using LSS and CMB data. Because for super-massive particles the velocity dispersion would be irrelevantly small, we choose to explore a broad range of masses, from 10^{-3} to 10^9 eV's. Using these limits and the 21-cm Cosmic Dawn observations, we propagate the phenomenology to explore their collisional cross-section with baryons, taking a velocity dependent interaction of the form $\sigma \propto v^{-4}$ and v^{-2} . Following these prescriptions, we pay particular attention to the constraints on the DM minicharge and the electric dipole moment.

For our exploration, we employ the simplest assumption for a generic DM momentum distribution, the Boltzmann or Gaussian function. This is not only simple but arguably the most physically motivated momentum distribution for DM. For example, thermal relics of Weakly Interacting Massive Particles (WIMPs) would obey classical Maxwell-Boltzmann statistics. On the other hand, if Axions or other Weakly Interacting Slim Particles (WISPs) were produced through a non-thermal injection or a phase transition, they would be described by a narrow Gaussian momentum distribution.

Throughout this paper we adopt the term *velocity dispersion* as the expectation value $\langle p/m \rangle$, weighted with an specific momentum distribution $f(p)$. For thermal relics, this is known as the *thermal velocity*. Our focus is on the primordial velocity dispersion of DM particles through the study of cosmological data in the linear regime.¹

The rest of this paper is organized as follows: in section 2 we briefly review the types of DM according to their mass and velocity dispersion. In section 3 we constrain the DM velocity dispersion today, evolving a non-interacting fluid described by a Gaussian momentum distribution. Then, in section 4 we connect our results with the mechanism of baryon-DM interactions proposed to cool down the baryonic gas. In section 5, the constraints found on the mass, velocity, and scattering cross-section are then translated to the DM minicharge and electric dipole moment. Our conclusions are summarized in section 6.

2. HOT, WARM, AND COLD DM

Before getting in details of our analysis, it is worth to briefly review general categories of DM. We do not intend a comprehensive summary but simply to articulate generic types of DM according to (not only their mass but) their velocity dispersion.

Cold DM is the most studied type of DM, for which the free-streaming scale is very small. Cold DM perturbations above this scale can be modeled as a perfect fluid with zero pressure or as a collisionless fluid with zero velocity dispersion. Beyond the Standard Model theories like Supersymmetry favor a large category of Cold DM particle candidates called WIMPs, with masses $1 \text{ GeV} \lesssim m_\chi \lesssim 3 \text{ TeV}$, which have been the target of

¹ On local scales, DM dynamics is influenced by gravitational infall, violent relaxation, and astrophysical feedback effects, so that, the DM velocity dispersion becomes much different than the primordial value. For example, in the Milky Way halo the velocity dispersion distribution deviates from the isotropic case, attaining, e.g., radial velocity dispersion values of $\sim 200 \text{ km s}^{-1}$ at the maximum (Bird et al. 2019).

most indirect and direct detection efforts (see e.g., [Gaskins 2016](#); [Liu et al. 2017](#)). If WIMPs were in thermal equilibrium in the early Universe, they obeyed a Boltzmann momentum distribution $\sim e^{-p^2/2M_w T_w}$, whose associated thermal velocity is $\langle p/M_w \rangle = \sqrt{8T_w/\pi M_w}$. This kind of heavy DM candidates should have decoupled very early in the radiation dominated era from a cosmic plasma with a large number of relativistic degrees of freedom (dof) $g_{w,\text{dec}}^*$. From the conservation of the specific entropy, we know that the WIMPs temperature is related to the radiation temperature as $T_w \propto (g_0^*/g_{w,\text{dec}}^*)^{2/3} T_\gamma^2/M$, where $g_0^* \sim 4$ are the relativistic dof today. It is pretty clear that for extremely large masses, the WIMPs temperature (and consequently their thermal velocity) would be extremely small as well.

Axions are another noteworthy Cold DM candidate. Originating from the Peccei-Quinn solution to the strong CP problem ([Peccei & Quinn 1977](#)), the QCD axion acquires a typical mass of $\sim 10^{-5} - 10^{-2}$ eV, near the QCD phase transition ([Marsh 2016](#)). At this time any interaction was already suppressed by the Peccei-Quinn scale; hence, axions would have been produced out-of thermal equilibrium and thus they are not subject to thermal velocities. A more general family of axion-like particles in a broad range of masses ($10^{-24} - 10^3$ eV) could be produced also non-thermally via the vacuum misalignment mechanism ([Ringwald 2012](#)). Furthermore, if by some mechanism axions are brought into thermal equilibrium, they would undergo a Bose condensation (BEC, [Sikivie & Yang 2009](#); [Erken et al. 2012](#)). In either case, axions shall be well described by a Boltzmann-like distribution $\sim e^{-p^2/\Delta p^2}$, where the momentum width Δp (extremely small for axion Cold DM) encodes the physics of the process leading to the non-thermal state².

Though being by far sub-dominant, Hot DM is the best-known component of DM because it is mainly composed of active neutrinos ([Abazajian & Kaplinghat 2016](#)). Neutrinos were in thermal equilibrium in the early Universe, obeying the Fermi momentum distribution in the relativistic limit $(e^{p/T_\nu} + 1)^{-1}$. Unlike for any other DM candidate, the decoupling temperature is fairly well known $T_{\nu,\text{dec}} \approx 1$ MeV ([Lesgourgues & Pastor 2006](#)). At that time only e^\pm and γ contributed to the relativistic dof, $g_{\nu,\text{dec}}^* = 10.75$. After decoupling, their temperature is proportional to the one of photons $T_\nu = (4/11)^{1/3} T_\gamma$, and then gets simply red-shifted. Neutrinos become non-relativistic at late epochs composing a small fraction of matter today $\Omega_\nu h^2 = \sum m_\nu/94$ eV. The neutrino thermal velocity is completely parametrized in

terms of their mass, $\langle p/m_\nu \rangle \approx 3.15 T_\nu/m_\nu \approx 150 (\text{eV}/m_\nu)$ km s⁻¹. The net effect of active neutrinos is to wash-out the small scale matter fluctuations and above the free-streaming wavenumber $k_{\text{fs}}(z=0) = 0.01 - 0.1 h$ Mpc⁻¹. For that reason, cosmological observations tightly constrain the sum of neutrino masses below the eV-scale.

If a small fraction of axions somehow thermalized (see e.g. [Archidiacono et al. 2013](#)), then they would obey a Bose distribution $(e^{p/T_a} - 1)^{-1}$. Thermal axions (and any other sub-eV thermal species) are also Hot DM candidates with a behavior close to active neutrinos.

Warm DM is an interesting intermediate phase, characterized by slow particles albeit not zero pressure, and consequently with non-negligible free-streaming scales. Sterile neutrinos are Warm DM candidates well motivated from theory and invoked by some anomalies in short-baseline oscillation data ([Lasserre 2014](#)). They can mix with active neutrinos but do not carry weak interactions ([Abbiendi et al. 2006](#)). In similarity to active neutrinos, sterile neutrinos are often assumed to decouple thermally while being relativistic, obeying the Fermi distribution $(e^{p/T_s} + 1)^{-1}$. In this case, the relic temperature is unknown but it should be proportional to the photon temperature too, $T_s = (g_0^*/g_{s,\text{dec}}^*)^{1/3} T_\gamma$, where g_0^* are the relativistic dof today.

Studying sterile neutrino mass bounds is a twofold task: from LSS considerations and from indirect DM searches. Assuming a specific value for $g_{s,\text{dec}}^*$ (for example 106.75 in the Standard Model and twice as much in Supersymmetry), the thermal velocity and free-streaming scale become completely specified by the mass m_s and its effects can be constrained with measurements of the MPS data (especially through the Ly α forest for the scales of interest), leading this to a lower-limit on m_s ([Abazajian 2017](#)). On the other hand, a fraction of sterile neutrinos is expected to decay rapidly leading to a source of mono-energetic photons with energy close to half of its mass. A hint of such a decay has been prompted by the discovery of an unidentified emission line at 3.5 keV in the stacked X-ray spectrum of galaxy clusters and galaxies (see [Abazajian 2017](#), and references therein).

The majoron (a scalar boson proposed to explain the *See-Saw* mechanism, [Chikashige et al. 1981](#)) is also a good Warm DM candidate. With properties and effects similar to sterile neutrinos, they can be modeled with a thermal Bose momentum distribution $(e^{p/T_J} - 1)^{-1}$, and a temperature $T_J = (g_0^*/g_{J,\text{dec}}^*)^{1/3} T_\gamma$.

In general, thermal relics are defined by the relativistic dof at the moment of their decoupling g_{dec}^* . Correspondingly, the thermal velocity is $\langle p/m \rangle = \sqrt{8T/\pi m}$ in the case of Boltzmann relics, $3.15 T/m$ in the case of

² BECs are commonly referred to as non-thermal states, albeit their physical origin is obviously thermal.

fermions, and $2.7 T/m$ in the case of bosons. Evaluated today, the thermal velocity can be expressed approximately equal for fermions and bosons,

$$v_{\text{th}} \approx 0.2 \left(\frac{g_0^*}{g_{\text{dec}}^*} \right)^{1/3} \frac{1 \text{ keV}}{m} \text{ km s}^{-1}, \quad (1)$$

where $T_{\text{cmb}} = 2.72 \text{ K}$ is implicit. An equivalent parametrization –often used for Warm DM– can be written indicating explicitly the DM abundance (Hogan & Dalcanton 2000; Bode et al. 2001),

$$v_{\text{th}} \approx 0.06 \left(\frac{\Omega_\chi h^2}{g_\chi} \right)^{1/3} \left(\frac{1 \text{ keV}}{m} \right)^{4/3} \text{ km s}^{-1}, \quad (2)$$

where g_χ are the DM particle dof. These two expressions are equivalent and hold for relativistic Fermi and Bose thermal species. Similar expressions can be obtained for Boltzmann relics, just by multiplying Eq. (1) by $\sqrt{x_d/2}$ and Eq. (2) by $e^{x_d/3}$; where $x_d \equiv m/T_d$ accounts for the precise time of DM kinetic decoupling.³

Non-thermal processes, however, are possible and play a crucial role in Warm DM models. For example, an important fraction of sterile neutrinos could be resonantly produced (RP, Abazajian 2017). RP sterile neutrinos are generated with small velocities, characterized by a sharp distribution peaked at small momenta. The average momentum reduction is not unique and depends on the specific mechanism under consideration. For instance, the Shi–Fuller mechanism (Shi & Fuller 1999) predicts an average reduction of $\langle p \rangle_{\text{min}} \sim 0.25 \langle p \rangle_{\text{thermal}}$ (Laine & Shaposhnikov 2008; Boyarsky et al. 2009a). But Bezrukov et al. (2018) proposed a model implying even smaller values. In any case, the bounds on the sterile neutrino mass (or equivalently, their velocity dispersion) become weaker in the case of resonant production compared to their thermal counterparts. Another possible source of non-thermal production is a late decay of heavy particles, inducing distortions to an otherwise thermal distribution (Cuoco et al. 2005). Lastly, Bose condensation (Rodríguez-Montoya et al. 2013) of at least a fraction of DM particles is another example of non-thermal processes, which would relax the current constraints on the DM mass and velocities.

³ Elastic scattering with SM species is usually responsible for keeping DM particles in thermal equilibrium. In some models, kinetic decoupling might be assumed to occur at $x_d \approx 1$ (Lesgourgues et al. 2013). On the other hand, WIMP co-annihilation numerical studies suggest that their freeze-out point is $x_f = m/T_f \approx 20-30$ (Roszkowski et al. 2018). In general x_f and x_d are separate unknown parameters but the uncertainty is one-sided because the freeze-out should typically precede the kinetic decoupling.

Actually, it is not the DM mass but more precisely its velocity dispersion that defines the free-streaming length,

$$\lambda_{\text{fs}}(z) = 2\pi \sqrt{\frac{2}{3}} \frac{\Delta v(z)}{H(z)}, \quad (3)$$

which determines the scale below which DM cannot remain gravitationally confined; or equivalently in Fourier space, the wavenumbers above which matter structures are *washed-out* from the MPS. The comoving free-streaming wavenumber $k_{\text{fs}}(z_{\text{nr}}) = 2\pi a(z_{\text{nr}})/\lambda_{\text{fs}}(z_{\text{nr}})$ provides a rough approximation to know the k 's below which the free-streaming effects are negligible, where z_{nr} denotes the time of non-relativistic transition. For thermal candidates the free-streaming scale depends on the mass and g_{dec}^* as they are given in equation (1). In the case of non-thermal candidates, their velocity dispersion (and consequently their free-streaming scale) depends on the specific model of DM production.

Now, irrespective of the precise nature of DM, their particles will be described by a momentum distribution denoted by $f(p)$. Whenever DM interactions are negligible, $f(p)$ evolves according to the Vlasov equation $df/dt=0$, whose perturbations in Fourier space read (Ma & Bertschinger 1995)

$$\dot{\Psi} - i \frac{q}{\epsilon_q} \Psi = - \left((\mathbf{k} \cdot \hat{\mathbf{n}}) \dot{\psi} + i \frac{\epsilon_q}{q} (\mathbf{k} \cdot \hat{\mathbf{n}}) \dot{\phi} \right) \frac{\partial \ln f}{\partial \ln q}, \quad (4)$$

where $q=ap$ is the comoving momentum magnitude, $\hat{\mathbf{n}}$ is the momentum unit vector, \mathbf{k} is the Fourier wave vector, and a is the scale factor. The dynamic variables are the scalar perturbations ψ , ϕ to the homogeneous Lemaitre-Friedman metric, a linear statistical perturbation Ψ to $f(p)$, and the comoving proper energy $\epsilon_q \equiv (q^2 + a^2 m_\chi^2)^{1/2}$. In general, equation (4) has to be solved as a Boltzmann-hierarchy of differential equations. This is the case for Hot and Warm DM, but not for Cold DM. In the limit $T \rightarrow 0$ or $\Delta p \rightarrow 0$, one can cut the Boltzmann hierarchy (see *e.g.*, Dodelson 2003; Mo et al. 2010) and the Vlasov equation (4) reduces to

$$\dot{\delta}_\chi + \theta_\chi = -\dot{h}/2 \quad \dot{\theta}_\chi + H \theta_\chi = 0, \quad (5)$$

where $\delta_\chi = \delta\rho_\chi/\bar{\rho}_\chi$ is the DM fluctuating over-density, and θ_χ is the peculiar velocity. In synchronous gauge, θ_χ is zero and Cold DM is evolved only through δ_χ . The results obtained from this approach are valid strictly within the linear regime, as such, Δv is scale-invariant and is interpreted as the primordial DM velocity dispersion.

Well inside the non-linear regime, DM particles are subject to violent processes depending on the scale and local environments (*e.g.* gravitational infall, astrophysical feedback effects, etc.), so that their phase-density

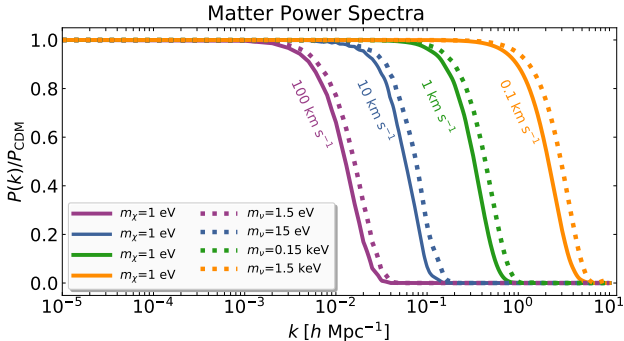


Figure 1. Distinct ratios of the MPS with respect to Cold DM. Same color indicate same velocity dispersion. Solid lines correspond to 1 eV-mass DM particles described by the Gaussian distribution f_χ , while dotted lines are thermal neutrinos described by the Fermi distribution. The neutrino thermal velocity is uniquely specified by its mass. In contrast, DM particles described with f_χ approach to Cold DM as $\Delta v_0 \rightarrow 0$, irrespective of their mass.

can be considerably modified. Although the latter is not our case of study, we mention that some interesting inferences have been attempted by comparing the primordial and coarse-grained DM phase-densities (Tremaine & Gunn 1979; Madsen 1991; Hogan & Dalcanton 2000; Boyarsky et al. 2009b).

3. GENERIC CONSTRAINTS ON THE DM VELOCITY DISPERSION

The only knowledge about the DM momentum distribution $f_\chi(p)$ is that it must be peaked at low momenta in order to describe non-relativistic, (almost-)pressureless matter. We argue that a Gaussian distribution is a good generic description because it represents a variety of DM scenarios, from heavy thermal relics to non-thermal distortions, and even phase-transitions. We implement the Gaussian momentum distribution

$$f_\chi(p) = \frac{n_\chi}{\pi^{3/2} \Delta p^3} \exp\left(-\frac{p^2}{\Delta p^2}\right) \quad (6)$$

in CLASS (Blas et al. 2011; Lesgourgues & Tram 2011), replacing the default Cold DM with this non-Cold DM module described by $f_\chi(p)$. Here Δp is the momentum width and $n_\chi = \int d^3p f_\chi(p)$ is the number density. Without regard to the (thermal or not) origin of DM, we can define a fiducial ‘temperature’ $T_\chi = \Delta p^2/2m_\chi$, in terms of which, we can write the velocity dispersion $\Delta v = \langle p/m_\chi \rangle = \sqrt{8T_\chi/\pi m_\chi} = 1.13 \Delta p/m_\chi$. Notice that the velocity dispersion gets linearly red-shifted $\Delta v = \Delta v_0 (1+z)$, being Δv_0 the value measured today.

As mentioned in §2, the DM description with equation (6) reduces to standard Cold DM in the limit $\Delta v \rightarrow 0$. This is reproduced in Figure 1, where we plot the MPS

ratio (over Cold DM) for fixed $m_\chi=1$ eV but different values of Δv_0 . These ratios progressively approach to 1 for smaller values of Δv_0 . An analogous effect is produced by a Fermi distribution that progressively approaches to Cold DM for masses in the keV-range. But we recall that the velocity dispersion (not the mass) regulates the free-streaming scale for a given DM model. In Figure 1 we show both Gaussian and Fermi cases for equivalent velocity dispersions, from which we notice that the Gaussian distribution causes slightly more suppression on the MPS than Fermi. Thus, we are showing that the Gaussian distribution $f_\chi(p)$ is a convenient description for DM because through its parameters it can cover hot, warm, and cold possible states of DM.

Our primary goal is to obtain observational constraints for Δv_0 using public data surveys such as Planck (Aghanim, N. et al. 2016; Ade, P. A. R. et al. 2016), Baryonic Acoustic Oscillations (BAO, Alam et al. 2017; Buen-Abad et al. 2018), and Red Luminous Galaxies from the Sloan Digital Sky Survey (SDSS, Tegmark et al. 2006). We employ MONTEPYTHON (Audren et al. 2013; Brinckmann & Lesgourgues 2018) to perform Bayesian estimations using $0 < \Delta v_0/\text{km s}^{-1} < 30$ as a prior. Although we have seen that the CMB and MPS are insensitive to the DM mass (when Δv_0 is varied independently), we choose to check for any marginal effect by splitting the analysis into six stages from sub-eV to GeV as indicated in Table 1. For the rest of the cosmological parameters, we use customary flat priors. Additionally, for any pair values of $\Omega_\chi h^2$ and m_χ , n_χ gets internally rewritten by CLASS in order to satisfy the equation $\Omega_\chi = m_\chi n_\chi/\rho_c$ (with ρ_c the critical density).

After a deep exploration, the standard cosmological parameters are constrained in concordance with standard reports (Ade et al. 2016). We find no significant degeneracies between Δv_0 and the standard cosmological parameters, suggesting an independent effect from our parametrization. As expected, the mass parameter m_χ is unconstrained when the velocity dispersion is varied independently. As it can be read from Table 1 and figure 2, the constraints on Δv_0 are not significantly different by comparing the six stages of mass-sampling. The Planck and BAO BOSS data constrain the free-streaming effects that would be caused by a large DM velocity dispersion (similarly to an increase on the effective number of relativistic species). But the most restrictive constraints on Δv_0 are obtained when the LSS data are included, because the free-streaming suppresses the MPS on small scales. Summarizing the results, our analysis shows that cosmological data constrain the DM velocity dispersion to

$$\Delta v_0 \lesssim 0.33 \text{ km s}^{-1} \quad (99\% \text{ CL}). \quad (7)$$

This translates to a lower bound on the epoch of DM non-relativistic transition, $z_{\text{nr}} \gtrsim 10^6$. But because $k \lesssim 0.2 \text{ h Mpc}^{-1}$ wavenumbers correspond to modes that entered the horizon at redshifts $z \lesssim 10^5$, the free-streaming effects of a DM species with $\Delta v_0 \ll 0.33 \text{ km s}^{-1}$ would not be noticeable at the scales of the LSS data used in our analysis.

In figure 2 we also mark the thermal velocity, using equation (1), due to active neutrinos and thermal axions; according to previous reports on their masses, $\sum m_\nu \lesssim 0.23 \text{ eV}$ (Ade et al. 2016) and $m_{a,\text{th}} \lesssim 0.67 \text{ eV}$ (Archidiacono et al. 2013). We also plot the thermal velocity given in equation (2), with $\Omega_\chi h^2 = 0.12$, and $g_\chi = 2$ (dark-red line). We should correct v_{th} in two ways: First, we have to take into account the uncertainties on the mass, which is the most unknown parameter, leading us to the error propagation $\delta v_{\text{th}} \approx 4/3 v_{\text{th}} (\delta m/m)$. Unfortunately, we do not count on any measurement of the DM mass; thus, we adopt a conservative choice for the mass error $\delta m = 0.3 m$ (roughly what it might be expected after a preliminary and speculative evidence of this parameter) that may help us for illustrative purposes. Second, we include a Shi-Fuller correction to relax the bounds in the case of resonant production of sterile neutrinos (light-red band). Additionally, we ought to account for the uncertainty on the details of kinetic decoupling (*e.g.* the value of g_{dec}^* or x_d , see text below Eq. 1), but for illustrative purposes, we just depict the thermal velocity as it is shown in equation (2). We also spot the mass constraint $m_J = 0.158 \pm 0.007 \text{ keV}$ re-

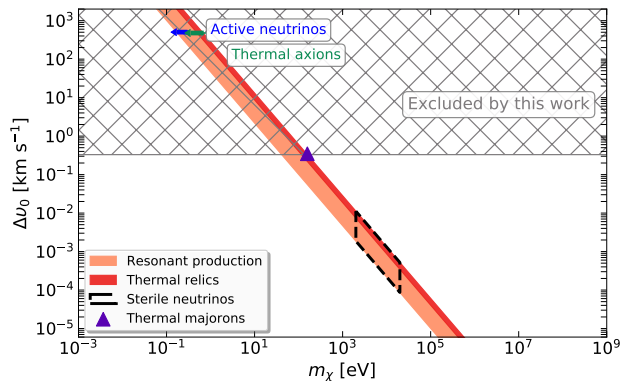


Figure 2. Constraints on the DM velocity dispersion after our analysis of the CMB and LSS data. The dark-red line shows thermal velocities for Warm DM using equation (2), while the light-red band is a 0.25 non-thermal correction (due to resonant production in the case of sterile neutrinos). Previous reports on sterile neutrino and thermal majorons are shown as candidates of Warm DM. Reports on Hot DM candidates such as active neutrinos and thermal axions are shown using equation (1).

ported for thermal majorons as a Warm DM candidate (Lattanzi et al. 2013). Thermally produced sterile neutrino bounds are still in debate, there is a controversy between lower bounds from cosmological data and upper bounds from diffuse X-ray emission (see these comprehensive reviews Adhikari et al. 2017; Boyarsky et al. 2018). In contrast to thermal relics, resonantly produced (RP) sterile neutrinos do not need large mixing angles with active neutrinos to match the required DM abundance. As a consequence, RP sterile neutrino decays into X-rays may be suppressed, thereby loosening the mass upper bound. Recent analyses of Ly- α forest data set a lower limit $m_s \gtrsim 5.3 \text{ keV}$ on thermally produced sterile neutrinos (Iršič et al. 2017, which is larger than previous determinations).⁴ Meanwhile, combined analyses of SDSS/BOSS and Ly- α forest data set a lower limit $m_s \gtrsim 3.5 \text{ keV}$ on RP sterile neutrinos (Baur et al. 2017). A noteworthy recent report based solely on the EDGES signal measured timing, sets a lower limit of $m_s \gtrsim 2 \text{ keV}$ (Safarzadeh et al. 2018). On the other hand, the non-observation of X-ray photons induced by the decay of sterile neutrinos sets an upper bound of $m_s \lesssim 20 \text{ keV}$ (Adhikari et al. 2017). All in all, we include in figure 2 (see black-dashed lines) mass constraints on both thermal and RP sterile neutrinos within $2 \text{ keV} < m_s < 20 \text{ keV}$, corresponding to a velocity dispersion within $5 \times 10^{-5} \text{ km s}^{-1} \lesssim v_0^s \lesssim 10^{-2} \text{ km s}^{-1}$.

Figure 2 displays a wide region of allowed m_χ and Δv_0 parameters; let us now place our bounds in context. We begin to recall that active neutrinos and thermal axions –as well as any other Hot DM species– are clearly discarded as the main source of DM. In the case of thermal DM (or non-thermal one with a correction of 0.25) keep in mind that the respective dark and light red bands bear large uncertainties in the mass and kinetic decoupling parameters, so we use them only for illustrative purposes. With that in mind, we might read that our bounds seem to disfavour thermal candidates (including non-thermal corrections) with masses below $\lesssim 40 \text{ eV}$. A previous report on thermal majorons (Lattanzi et al. 2013) is at the edge but within of our 99% CL bounds. Previous reports on thermal (Iršič et al. 2017) and resonant (Baur et al. 2017) sterile neutrinos are well below our 99% CL boundary. Notice again that our bounds do not exclude any DM mass from 10^{-3} to 10^9 eV 's. Indeed, Warm ($0 < \Delta v_0 \lesssim 0.33 \text{ km s}^{-1}$) and Cold ($\Delta v_0 = 0$) DM candidates are well allowed by our constraints, irrespective of their mass.

⁴ Notice that these constraints are still subject to uncertainties on the thermal evolution of the Intergalactic Medium.

Table 1. Bounds on the Dark Matter velocity dispersion from the six mass-sampling stages of the analysis.

		Stage 1	Stage 2	Stage 3	Stage 4	Stage 5	Stage 6
		$10^{-3} - 10^{-1}$ eV's	$10^{-1} - 10^1$ eV's	$10^1 - 10^3$ eV's	$10^3 - 10^5$ eV's	$10^5 - 10^7$ eV's	$10^7 - 10^9$ eV's
P		1.32	1.31	1.33	1.34	1.31	1.33
PB	$\Delta\nu_0$ [km s $^{-1}$] \lesssim	1.28	1.27	1.26	1.25	1.26	1.25
PBS		0.32	0.32	0.32	0.33	0.32	0.33

NOTE—Upper limits at 99% CL. The prior on the velocity dispersion is $0 < \Delta\nu_0/\text{km s}^{-1} < 30$ for every stage of the analysis. The datasets are denoted with *P*: Planck, *PB*: Planck + BAO BOSS, *PBS*: Planck + BAO BOSS + SDSS DR4 LRG.

4. ROLE OF DM VELOCITY DISPERSION ON THE 21-CM SIGNAL

In many studies of the 21-cm Cosmology, it is customary to fix the DM mass to the WIMPs scale, whose corresponding thermal velocity is nearly zero. But from the previous section we see that a vast variety of DM candidates could involve a significant velocity dispersion while still reproducing the observed LSS and CMB spectra. Now we are going to use the constraints of Figure 2 in order to explore the $\Delta\nu_0$ effects on the interpretation of the EDGES measurements.

EDGES probes the epochs after primordial recombination and before the formation of the first luminous sources. During these epochs, the baryonic gas is mainly composed of neutral hydrogen with total spin $S=0$ (proton/electron anti-parallel spins). When an atom in the parallel state ($S=1$) realigns its spins, a photon is emitted with an energy $E_{21}=5.87 \mu\text{eV}$, equivalent to a wavelength of 21 cm. The 21-cm signal is the observed brightness temperature with respect to the photon background (for a comprehensive review see: Furlanetto et al. 2006; Morales & Wyithe 2010; Pritchard & Loeb 2012),

$$T_{21}(z) = (27 \text{ mK}) \frac{x_{\text{HI}} \Omega_b h^2}{0.023} \left(1 - \frac{T_\gamma(z)}{T_s(z)}\right) \left(\frac{0.15}{\Omega_m h^2} \frac{1+z}{10}\right)^{1/2}. \quad (8)$$

Here, x_{HI} (≈ 1 during the epoch of cosmic dawn) is the fraction of neutral hydrogen and Ω_b is the baryon abundance. T_s is called the ‘spin temperature’, which defines the relative population of the two spin levels $n_1/n_2 \equiv 3e^{-E_{21}/T_s}$, it can be parametrized in terms of the baryon and photon temperatures, $T_b(z)$ and $T_\gamma(z)$, and the stimulated Ly- α emission (Chen & Miralda-Escudé 2004). In the limit of full Ly- α coupling, we take $T_s = T_b$ (Madau et al. 1997). The 21-cm signal is then redshifted till the band of radio-frequency today. The EDGES collaboration reported $T_{21} = -0.5^{+0.2}_{-0.5}$ K (99% C.L.) in a redshift range $13 \lesssim z \lesssim 22$, centered at $z \approx 17$ (or a frequency of 78 MHz).

Some aspects of the reported absorption profile are peculiar and need to be explained: the early redshift

range with their implications for star formation (Madau 2018; Mirocha & Furlanetto 2018), the flat shape of the profile (Venumadhav et al. 2018), and the unanticipated deep trough. Assuming only standard physical scenarios, the maximum value of the absorption trough would be $T_{21} \approx -0.2$ K, *i.e.* the measurement is at least twice the standard expectation. Given that T_{21} depends on the ratio T_γ/T_s , two main explanations are currently discussed to enhance the absorption: *i*) An excess of radiation injected from DM-annihilations, black holes, or any other astrophysical source (see *e.g.* Chianese et al. 2018; Clark et al. 2018; Feng & Holder 2018; Sharma 2018). *ii*) A cooling mechanism of baryons through interactions with DM (see *e.g.* Dvorkin et al. 2014; Tashiro et al. 2014; Muñoz et al. 2015; Barkana 2018; Berlin et al. 2018; Slatyer & Wu 2018; Xu et al. 2018). It should also be mentioned that the EDGES findings are being argued to be due to systematics related to residual foregrounds (Hills et al. 2018). Thus, the EDGES observations require confirmation from similar experiments like SCI-HI (Voytek et al. 2014), LEDA (Bernardi et al. 2016), and SARAS 2 (Singh et al. 2017). Ultimately, the EDGES results open a rich discussion pointing to new physics and novel phenomenological frameworks.

Here we focus on the baryon-DM interaction hypothesis, assuming a velocity-dependent scattering cross-section $\sigma(v) = \sigma_0 v^n$, where $v = |\mathbf{v}_\chi - \mathbf{v}_b|$ is the relative velocity between two particles⁵. We choose to explore two cases of low-energy enhanced interactions, namely $n = -4$ and $n = -2$, which are motivated by models of minicharge and electric dipole moment, respectively. Other cases of n have been studied elsewhere, (see *e.g.*, Dvorkin et al. 2014; Slatyer & Wu 2018; Xu et al. 2018).

The thermal evolution of baryons and DM involves the baryon and DM temperatures, $T_b(z)$ and $T_\chi(z)$; the energy transfer between baryons and DM, Q_b and Q_χ ; and the relative bulk velocity $V_{\chi b}$. The full formalism

⁵ It is also customary to use a parameter σ_1 that relates to σ_0 as $\sigma_0 = ([1 \text{ km s}^{-1}]/c)^4 \sigma_1$.

can be read up on [Dvorkin et al. \(2014\)](#), [Tashiro et al. \(2014\)](#), or [Muñoz et al. \(2015\)](#); let us just discuss the baryon-DM energy transfer,

$$\dot{Q}_b^{(n)} = \sum_{t=e,p} \frac{f_{\text{dm}} \rho_\chi \sigma_0 m_t}{(m_t + m_\chi)^2} \left(\frac{(T_\chi - T_b) S_n(r_t)}{u_t^{-(n+1)}} + \frac{m_\chi F_n(r_t)}{V_{\chi b}^{-(n+3)}} \right), \quad (9)$$

where t refers to the proton or electron, f_{dm} is the fraction of DM interacting with baryons, $u_t = \sqrt{T_b/m_t + T_\chi/m_\chi}$ is the thermal width of the relative bulk velocity, and $r_t = V_{\chi b}/u_t$. Notice that the first term subtracts energy from baryons as long as $T_\chi < T_b$. This cooling term is suppressed by the functions $S_n(r_t)$, where $S_{-4}(r_t) = \sqrt{2}e^{-r_t^2/2}/\sqrt{\pi}$ and $S_{-2}(r_t) = 2\text{Erf}(r_t/\sqrt{2})/r_t$. The second term transforms the mechanical energy into heating to both baryons and DM, where $F_{-4}(r_t) = \text{Erf}(r_t/\sqrt{2}) - \sqrt{2}r_t e^{-r_t^2/2}/\sqrt{\pi}$ and $F_{-2}(r_t) = \text{Erf}(r_t/\sqrt{2}) - r_t^{-2} F_{-4}(r_t)$. This term can spoil the cooling mechanism unless the velocity ratio r_t is small ($V_{\chi b} \ll u_t$), or the DM mass is small ($m_\chi \ll m_t$).

The hypothesis of baryon-DM scattering has been extensively studied using CMB and MPS observables (the same observables that we just used to constrain Δv_0), which are made of modes that entered the horizon at $z \sim 10^3 - 10^5$ (with the Ly- α forest it is possible to probe beyond $z \gtrsim 10^6$). At those early times, the overall effect of baryon-DM interactions would mimic an increase of the baryonic budget; consequently, both the CMB and MPS would become damped on small scales ([Chen et al. 2002](#); [Dvorkin et al. 2014](#)). This effect is actually a very good probe for the strength of baryon-DM scattering and previous studies have reported tight upper limits: $\sigma_0 \lesssim 10^{-41} \text{ cm}^2$ for $n = -4$ ([Slatyer & Wu 2018](#); [Xu et al. 2018](#); [Boddy et al. 2018](#)), and $\sigma_0 \lesssim 10^{-33} \text{ cm}^2$ for $n = -2$ ([Xu et al. 2018](#); [Boddy et al. 2018](#)).

On the other hand, the precise fraction of interacting DM is still in debate (see *e.g.* [Dolgov et al. 2013](#); [Dolgov & Rudenko 2017](#)). According to constraints derived from the CMB, f_{dm} might be expected below the fractional uncertainty of the baryon energy density ([Kovetz et al. 2018](#)). Besides, in order to avoid other astrophysical constraints, a small f_{dm} might be necessary as well ([Chuzhoy & Kolb 2009](#); [McDermott et al. 2011](#)). In the following discussion we consider $f_{\text{dm}} = \{1, 0.1, 0.01\}$ only for exploratory purposes.

Taking into account the smallness of σ_0 and f_{dm} from linear Cosmology, the baryon-DM interactions would have little impact on the distribution of DM velocities and its dispersion should evolve as $\Delta v(z) = (1+z)\Delta v_0$ right after photon decoupling. Afterwards ($z \lesssim 10^3$), the low-velocity enhanced scattering ($n = -4$ or $n = -2$) cause a late-time coupling between DM and baryons.

Although the non-interacting fraction will preserve an adiabatic dilution ($\Delta v_{\text{NI}} \sim 1+z$), the interacting fraction will be heated and its velocity dispersion $\Delta v_t(z)$ will not follow a linear evolution with z . In fact, $\Delta v_t(z)$ can only be computed numerically after the solution to the heat transfer equations involving (9). Thus, when interactions are effective, the average DM velocity dispersion is

$$\Delta v_{\text{av}}(z) = f_{\text{dm}} \Delta v_t(z) + (1 - f_{\text{dm}}) \Delta v_{\text{NI}}(z). \quad (10)$$

Given that the DM velocity dispersion is constrained directly by the effective amount of matter needed for LSS formation, the constraints found in the previous section should approximately hold even in the interacting case. Indeed, the upper-limit in equation (7) can be used as an initial condition,

$$\Delta v_{\text{av}}(z) \lesssim (1+z)\Delta v_0, \quad \text{at } z \approx 10^3. \quad (11)$$

Now, in order to solve the 21-cm thermal dynamics, we can substitute $T_\chi = (\pi/8)m_\chi \Delta v_{\text{av}}^2$ in the thermal width u_t , starting the integration at an epoch much before the Cosmic Dawn ($z \sim 10^3$), and use equations (11) and (7) to define a set of initial conditions.

Let us intuitively discuss the kinematics involved in the 21-cm thermal evolution and heating transfer. We already mentioned below equation (9) that there is a competition between the cooling mechanism (first term) and the mechanical heating (second term). The most obvious way to enhance the baryon cooling is having a large σ_0 , albeit possibly conflicting with cosmological bounds. Also obvious is the fact that the colder DM initially is, the easier for it to absorb heat from baryons; this is easily seen in equation (9) because a smaller thermal width u_t enhances the cooling term. Contrarily, the mechanical heating can overcome the cooling mechanism in some cases. For example, particles as heavy as 1-10 GeV would need $\sigma_0 \gtrsim 10^{-39} \text{ cm}^2$ in order to explain the EDGES signal, even in the case of $f_{\text{dm}} = 1$ and zero initial DM velocity dispersion ([Barkana 2018](#)); clearly conflicting with cosmological bounds. The mechanical heating can be suppressed though, if the DM mass is small enough ($m_\chi \ll m_t$) and/or the velocity ratio r_t is small ($V_{\chi b} \ll u_t$). The latter has also been identified as a necessary condition to maintain linearity in the perturbative Boltzmann equations (see *e.g.* [Boddy & Gluscevic 2018](#); [Slatyer & Wu 2018](#); [Kovetz et al. 2018](#); [Boddy et al. 2018](#)).

The DM mass is a very interesting parameter in this framework. Given that the absorbed heat is distributed among the number of interacting DM particles, the cooling mechanism seems to be easier if the DM mass is small. In other words, the lighter DM is, the transferred

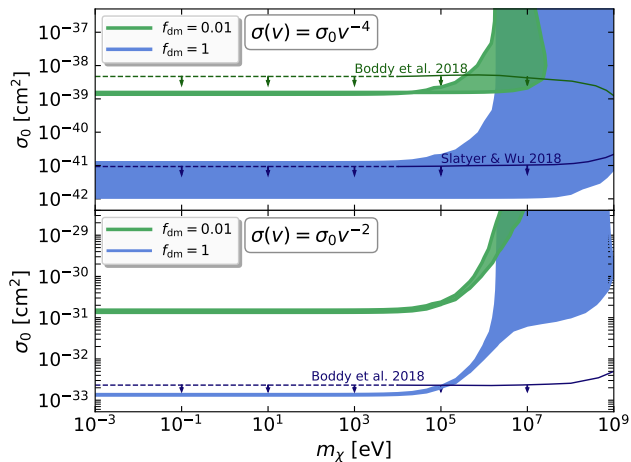


Figure 3. Constraints on the baryon-DM scattering cross-section required to explain EDGES signal, reported in terms of the mass and marginalized over $\Delta\nu_0$. The blue (green) region represents the 99% CL for $f_{\text{dm}} = 1.0$ ($f_{\text{dm}} = 0.01$). Each solid line represents the Planck upper bounds on the cross section from (Slatyer & Wu 2018) and (Boddy et al. 2018) (blue for $f_{\text{dm}} = 1.0$ and green for $f_{\text{dm}} = 0.01$); dashed lines are an extrapolation to smaller DM masses.

energy is spread out over more particles, which could be understood as a more efficient thermal reservoir than in the heavier case.

We also identify a couple of differences between the two types of scattering: *i*) For $n = -4$, the electron-DM interaction is only relevant if DM particles are not cold, otherwise σ_0 is dominated by proton-DM interactions. *ii*) On the other hand, for $n = -2$, the scattering is electron dominated for $m_\chi \lesssim 5 \times 10^5$ eV (even for Cold DM particles); above that mass, the interaction is proton dominated.

Now we can proceed to fit the 21-cm temperature appearing in equation (8) to the EDGES measurement. In practice, for each pair of $\Delta\nu_0$, m_χ fixed values, we solve for σ_0 to recover $T_{21}(z = 17) \approx -0.5$ K. Figure 3 displays the resulting allowed regions for σ_0 and m_χ marginalized over $\Delta\nu_0$, for $n = -4$ and $n = -2$, and the fractions $f_{\text{dm}}=1$ and 0.01. Notice that if the initial thermal width u_t is large, it will suppress the cooling term in equation (9); such a suppression can only be compensated by σ_0 , requiring stronger baryon-DM interactions. The larger values of σ_0 in Figure 3 are clearly in conflict with typical cosmological bounds⁶. Indeed, with a tighter bound on $\Delta\nu_0$ resulting from small-scale LSS data like *e.g.* Ly- α forest, the allowed space for σ_0 would shrink below

⁶ Yet, recall that current cosmological bounds have been mainly focused on DM masses above MeV's.

the current cosmological bounds. For masses above 0.1 MeV's, the explanation of the EDGES measurement requires heavy DM particles to be initially very cold. But lighter DM particles are much less restricted on their velocity dispersion initial conditions, which is due to the aforementioned better cooling efficiency of light-DM particles.

5. ELECTROMAGNETIC PROPERTIES OF DM?

In this section we discuss the physical motivation for the $n = -4$ and $n = -2$ scattering cases, relating them to the electric minicharge ϵ and the electric dipole moment \mathcal{D} of DM, respectively.

5.1. Minicharge

The possible existence of new particles endowed with a small electric charge $q_\chi = \epsilon e$ (with e the electron charge and $\epsilon \ll 1$) is well motivated from simple extensions of the Standard Model that include a hidden sector with an $U'(1)$ unbroken gauge symmetry (Holdom 1986; Foot et al. 1990). The small effective charge is a byproduct of the kinetic mixing between hidden photons associated with $U'(1)$ and ordinary photons. Then, fermions in the hidden sector charged under $U'(1)$ can couple to ordinary photons via q_χ . If there were light charged scalars in the hidden Higgs sector, they would also acquire a tiny charge q_χ due to the photon mixing (Melchiorri et al. 2007; Ahlers et al. 2008; An et al. 2013). In some models, even neutrinos are explicitly allowed to acquire a small charge (Foot et al. 1990; Vinyoles & Vogel 2016). It turns out quite intuitive to think of Minicharged Particles (MCPs) to account for at least a fraction of the DM (Goldberg & Hall 1986). Indeed, MCPs are often quoted within the group of WISP-DM candidates (Jaeckel & Ringwald 2010; Ringwald 2012), including dark photons, majorons, axions, and axion-like particles.

The longstanding question about MCPs has led to several laboratory searches, like the experiments at the SLAC National Accelerator Laboratory, uniquely designed to detect MCPs (Prinz et al. 1998; Badertscher et al. 2007; Gninenko et al. 2007; Batell et al. 2014) that have set an upper bound $\epsilon \lesssim 10^{-5}$ in the 0.1 to 100 MeV mass range. Collider precision tests have set bounds going down to $\epsilon \lesssim 5 \times 10^{-4}$ (Davidson et al. 2000) for masses below 100 keV. Meanwhile, astrophysical and cosmological environments represent advantageous laboratories as many of them are sensitive to the effects of MCPs. For instance, Big Bang Nucleosynthesis (BBN) sets the condition $\epsilon \lesssim 10^{-8}$ (Mohapatra & Rothstein 1990) in order to prevent late thermalization of \lesssim MeV particles. Otherwise, DM would contribute with extra relativistic dof,

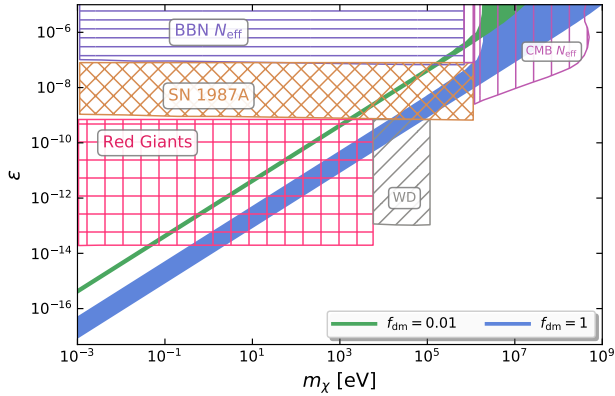


Figure 4. Constraints on the DM minicharge required to explain the EDGES signal. The blue (green) region represents our 99% CL constraints for $f_{\text{dm}} = 1$ ($f_{\text{dm}} = 0.01$) that are consistent with our bound (7) on the DM velocity dispersion. Bounds on MCPs from the early Universe and stellar physics are also shown (see text for references). The CMB- N_{eff} bound applies only to the model that explicitly includes the hidden photon relativistic dof.

which are tightly constrained to $N_{\text{eff}} = 2.94 \pm 0.38$ (Cyburt et al. 2016). If one counts the extra relativistic dof due to the hidden photons, then, the CMB bounds on N_{eff} also place constraints on the MCP parameter space (see e.g., Vinyoles & Vogel 2016; Barkana et al. 2018).

The strongest bounds on minicharge come from *the energy-loss argument*, alluding to the escape of these particles from the core of stars (Raffelt 1996). Excitations of the dense electron-proton plasma (also called plasmons) can decay into MCPs; if the charge is low enough ($\epsilon \lesssim 10^{-8}$, Davidson et al. 2000), they propagate freely through the plasma and escape from the star (Vinyoles & Vogel 2016). The dissipation of energy should modify the usual stellar evolution, thus limiting the plasmon decay-rate into MCPs, and hence constraining ϵ . Combining studies of White Dwarfs (WD), Red Giants (RG), the Super Nova 1987-A (SN87A), and the Sun (among others), indicate that $\epsilon \lesssim 2 \times 10^{-14}$ (Davidson et al. 2000; Vinyoles & Vogel 2016; Chang et al. 2018, see also Figure 4).

In the DM mass range of this work (10^{-3} - 10^9 eV), the DM particle number density is always comparable or much larger than baryons. Then, we should consider the cross-section due to a baryon propagating in an MCP plasma (McDermott et al. 2011),

$$\sigma_0 = \frac{2\pi\alpha^2\epsilon^2\xi}{\mu_{\chi t}^2}, \quad (12)$$

where α is the fine-structure constant and $\mu_{\chi t}$ is the reduced mass between the DM and the baryon (proton or electron). The Debye logarithm $\xi =$

Table 2. Bounds on the DM minicharge

f_{dm}	m_χ	ϵ
1	$10^{-3} - 2$ eV	$8 \times 10^{-18} < \epsilon < 2 \times 10^{-14}$
0.1	$10^{-3} - 0.4$ eV	$5 \times 10^{-17} < \epsilon < 2 \times 10^{-14}$
0.01	$10^{-3} - 0.05$ eV	$4 \times 10^{-16} < \epsilon < 2 \times 10^{-14}$

NOTE—Bounds on ϵ are directly read from Fig. 4.

$\log(9T_\chi^3/(4\pi\alpha^3\epsilon^4n_\chi))$, which regulates the screening of the interaction by the plasma, can be approximated in this case to $\xi \approx 93 - 4\log(10^{14}\epsilon \text{ (eV}/m_\chi))$. Given that MCPs cannot interact with neutral atoms, the energy transfer in equation (9) gets suppressed by the fraction of free electrons.

We can now obtain minicharge bounds by inserting equation (12) into the heat transfer equation (9), this is depicted in Figure 4. Notice that in order to simultaneously explain the EDGES signal and avoid stellar bounds, the DM mass needs to be towards the ultra-light regime. From the non-excluded m_χ - ϵ window, some bounds on the DM minicharge are listed in Table 2, according to three values of f_{dm} . Notice once again that a tighter bound on $\Delta\nu_0$ would result in a reduced allowed space for ϵ .

Incidentally, notice that the scattering due to MCPs is dominantly incoherent for our studied range of masses. This is due to the smallness of ϵ , causing the MCP's mean free path $\ell_\chi = (\sigma(v)n_\chi)^{-1}$ to be extremely large compared to the energy-exchange length $\lambda_{\chi b} = (\mu V_{\chi b})^{-1}$. Despite the apparently high densities at lower masses (e.g. for $z = 20$ and $m_\chi = 1$ eV, $n_\chi \sim 10^{10} \text{ cm}^{-3}$), the smallness of ϵ makes the MCPs a rarefied plasma. This might not be the case for ultra-light DM candidates. A minicharge as small as $\epsilon \sim 10^{-14}$ will be enough to cause ($\ell_\chi < \lambda_{\chi b}$) a scattering dominantly coherent for $m_\chi \ll 10^{-6}$ eV.

5.2. Electric dipole moment

Following the same spirit of MCPs, a type of neutral DM possessing an electric dipole moment (EDM) \mathcal{D} has been targeted for direct detection (Pospelov & ter Veldhuis 2000; Sigurdson et al. 2004, 2006)⁷. These particles can only be Dirac fermions in order to have a permanent dipole moment. It is customary to report \mathcal{D} in units of the Bohr magneton $\mu_B = e\hbar/2m_e = 1.93 \times 10^{-11} e \text{ cm}$.

⁷ Magnetic dipole moments (MDMs) \mathcal{M} have been experimentally targeted as well. Here we do not consider MDMs because they produce a velocity independent scattering ($n = 0$) with baryons (see e.g. Sigurdson et al. 2006).

BBN sets an upper bound, $\mathcal{D} \lesssim 5.2 \times 10^{-12} \mu_B$, in order to avoid late thermalization of particles below a few MeV's (Sigurdson et al. 2004). In the sub-GeV mass range, Collider Physics is the most sensitive probe to DM-EDM through radiative corrections to the W boson mass, which sets a mass independent upper limit at $\mathcal{D} \lesssim 1.6 \times 10^{-5} \mu_B$, and from perturbative constraints from corrections to Z-pole observables, requiring that $\mathcal{D} \lesssim 3.7 \times 10^{-5} \mu_B$ (Sigurdson et al. 2004). Stellar Physics constrain the neutrino magnetic dipole moment from the energy-loss argument discussed above. These constraints also apply to DM particles coupling to photons through an EDM. Accordingly, the most stringent astrophysical limits correspond to the Sun, WD, RG, and SN87A, implying $\mathcal{D} \lesssim 2 \times 10^{-12} \mu_B$ (Bertolami 2014; Kadota & Silk 2014; Arceo-Díaz et al. 2015; Cañas et al. 2016).

Our bounds on σ_0 computed with a v^{-2} dependence (as shown in Figure 3) can be translated to \mathcal{D} , according to (Sigurdson et al. 2004),

$$\sigma_0 = 2\alpha\mathcal{D}^2. \quad (13)$$

From the results depicted in Figure 5, we can see that the EDM needed to explain the EDGES measurement in the mass range 10^{-3} – 10^9 eV is already discarded by the BBN constraints and the measurements of the W boson mass in colliders.

As discussed above in the case of MCPs, the scattering through an EDM is also dominated by incoherent scattering in the mass range 10^{-3} – 10^9 eV. For example, if $\mathcal{D} = 10^{-4} \mu_B$, the scattering would be coherent ($\ell_\chi < \lambda_{\chi b}$) for $m_\chi \ll 10^{-6}$ eV. For an EDM as small as

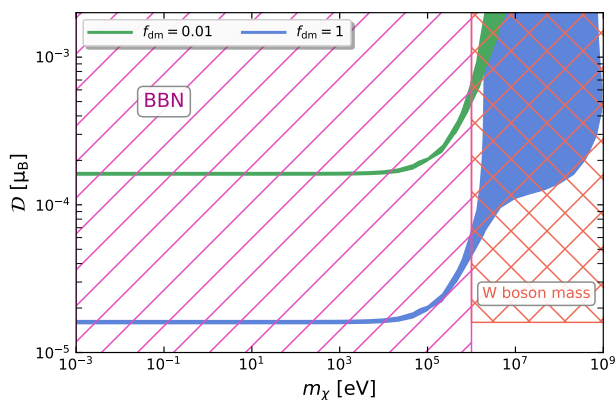


Figure 5. Constraints on the DM electric dipole moment required to explain the EDGES signal, along with the region already excluded by BBN and collider experiments. The blue (green) region represents the 99% CL region consistent with our constraints on the DM velocity dispersion for $f_{\text{dm}} = 1$ ($f_{\text{dm}} = 0.01$).

$\mathcal{D} = 10^{-12} \mu_B$, the scale of coherent scattering is pushed down to $m_\chi \ll 10^{-14}$ eV.

6. CONCLUSIONS

While the mass is quite an unknown aspect of DM, its velocity dispersion is a physical property much less studied. It is not uncommon to think that the DM relic velocity is either necessarily zero (assuming Cold DM) or thermally suppressed by the particle mass (in Warm DM models), like in equations (1) and (2). Nevertheless, as we have reviewed, there might be plenty of non-thermal mechanisms that would cause finite velocity dispersions, to some degree disentangling velocity and mass. Here, we have constrained a wide region of the m_χ – Δv diagram (Fig. 2) by means of the linear regime of matter perturbations and using current CMB and LSS data. Our analysis provides useful upper limits to the DM velocity dispersion, listed in Table 1 and summarized in equation (7). In general, we have shown that DM particles can be considered as Warm or Cold DM depending on their actual velocity dispersion, irrespective of their mass.

As expected, active neutrinos and thermal axions (Hot DM) are ruled out as the main source of DM. Thermal majorons are found barely allowed by our constraints, suggesting the need for further scrutiny with CMB and LSS data, and possibly accounting for their non-thermal corrections. Candidates for thermal DM are allowed above ~ 100 eV's by our constraints, while they are discarded for $m_\chi \lesssim 40$ eV's, even after considering non-thermal corrections. Resonantly produced sterile neutrinos and other non-thermal DM candidates are well inside our bounds. Very light ($\ll 1$ keV) DM particles are allowed by our constraints as long as their velocity dispersion concurs with our bound in (7). This motivates a deeper study of non-thermal production mechanisms like those briefly discussed in §2. Heavy thermal candidates are well below our velocity constraints.

Our bound (7) on the DM velocity dispersion is mainly limited by the maximum wavenumber (0.2 h Mpc^{-1}) contained in the SDSS DR4 LRG data. This motivates further studies using LSS data at smaller scales like those from the Ly- α forest, which can extend our analysis down to $k \lesssim 5 \text{ h Mpc}^{-1}$ and improve our constraints at least by an order of magnitude.

The DM velocity dispersion is a key ingredient of the 21-cm dynamics at the epoch of the Cosmic Dawn. If the anomaly in the absorption profile measured by EDGES is to be explained by a baryon-DM interaction, the T_{21} -signal by itself is not enough to constrain both the DM relic velocity and the baryon-DM scattering cross-section. Hence, it is of great importance to investigate Δv using independent techniques and sets of data.

In order to overcome the highest allowed velocities and henceforth ensure an efficient baryon-cooling, the values of σ_0 would need to be accordingly larger (as depicted in Figure 3). However, the largest σ_0 -values are in conflict with previous bounds (Slatyer & Wu 2018; Xu et al. 2018; Boddy et al. 2018) obtained from CMB and LSS data. This means that if DM particles are very heavy ($m_\chi \gg 1$ MeV), they ought to be initially really cold in order to explain the EDGES observation. If DM particles are very light ($m_\chi \ll 1$ keV), they do not seem to have tight restrictions on their initial velocities – other than (7) – in order to explain both early and late cosmological data. Yet, we speculate that such very-light DM scenarios would in turn need a very early cooling mechanism (like those discussed in §2) in order to attain velocities much smaller than thermal candidates.

We conclude that the $\Delta\nu_0 > 0$ allowed values found after our analysis can surely play a major role in the phenomenology of baryon-cooling. Once again, this motivates further studies with Ly- α forest or other small-scale LSS data, which could tighten the allowed parameter space for the baryon-DM scattering cross-section and minicharge (see figures 3 and 4).

Assuming that the $n = -4$ and $n = -2$ types of scattering are due respectively to MCPs and EDMs, our constraints on σ_0 translate to novel bounding areas for ϵ and \mathcal{D} , which are modified by our constraints on $\Delta\nu_0$. This effect is interesting in general for direct detection experiments at the low-energy end, whose typical targets are WISPs (Jaeckel & Ringwald 2010; Ringwald 2012). In this direction of research, a more complete and detailed sampling of the $(m_\chi, \Delta\nu_0, \sigma_0)$ parameter

space would be needed. In particular, the mass parameter space should be explored considering that the interacting and non-interacting DM fractions may be made of particles with different masses. This characterization will involve explicitly collisional terms in the baryon and DM Boltzmann equations, and a Boltzmann hierarchy of differential equations. Clearly, the former study would be very interesting and represents one way to improve our analysis.

On a side note, we briefly mentioned the mass-scale of incoherent/coherent scattering for MCPs and EDMs. We lastly say that in the latter case, the continuum nature of DM ought to be taken into account in close similarity to scale-invariant scenarios (Katz et al. 2016). Moreover, the associated multi-body interaction might imply a scattering driven by higher-order multipoles, possibly the anapole, quadrupole, or the DM polarizability (Pospelov & ter Veldhuis 2000; Ovanesyan & Vecchi 2015).

The authors thankfully acknowledge the computer resources provided by the Laboratorio Nacional de Supercomputo del Sureste de México, CONACYT network of national laboratories. This project was possible owing to partial support from CONACYT research grants 237004, 490769, F.C. 2016/1848, and FORDECYT-297324. V.A-R. acknowledges partial support from the project CONACyT CB285721. We also thank Tracy Slatyer, Cora Dvorkin, R.E. Sanmiguel, and J.B. Muñoz for interesting discussions. We especially want to thank an anonymous Referee for a critical review that has led to a significant improvement of our paper.

REFERENCES

- Abazajian, K. N. 2017, PhR,
doi:10.1016/j.physrep.2017.10.003.
<https://doi.org/10.1016/j.physrep.2017.10.003>
- Abazajian, K. N., & Kaplinghat, M. 2016, ARN&PS, 66, 401.
<https://doi.org/10.1146/annurev-nucl-102014-021908>
- Abbiendi, G., et al. 2006, PhR, 427, 257 . <http://www.sciencedirect.com/science/article/pii/S0370157305005119>
- Ade, P. A., Aghanim, N., Arnaud, M., et al. 2016, A&A, 594, A13. <https://doi.org/10.1051/0004-6361/201525830>
- Ade, P. A. R., Aghanim, N., Arnaud, M., et al. 2016, A&A, 594, A15. <https://doi.org/10.1051/0004-6361/201525941>
- Adhikari, R., Agostini, M., Ky, N. A., et al. 2017, JCAP, 2017, 025.
<http://stacks.iop.org/1475-7516/2017/i=01/a=025>
- Aghanim, N., Akrami, Y., Ashdown, M., et al. 2018, arXiv:1807.06209. <https://arxiv.org/abs/1807.06209>
- Aghanim, N., Arnaud, M., Ashdown, M., et al. 2016, A&A, 594, A11. <https://doi.org/10.1051/0004-6361/201526926>
- Ahlers, M., Jaeckel, J., Redondo, J., & Ringwald, A. 2008, PhRvD, 78, 075005.
<https://link.aps.org/doi/10.1103/PhysRevD.78.075005>
- Alam, S., Ata, M., Bailey, S., Beutler, F., et al. 2017, MNRAS, 470, 2617.
<http://dx.doi.org/10.1093/mnras/stx721>
- An, H., Pospelov, M., & Pradler, J. 2013, PLB, 725, 190 .
<https://doi.org/10.1016/j.physletb.2013.07.008>
- Arceo-Díaz, S., Schröder, K.-P., Zuber, K., & Jack, D. 2015, Astropart. Phys., 70, 1 . <http://www.sciencedirect.com/science/article/pii/S0927650515000468>
- Archidiacono, M., Hannestad, S., Mirizzi, A., Raffelt, G., & Wong, Y. Y. 2013, JCAP, 2013, 020.
<http://stacks.iop.org/1475-7516/2013/i=10/a=020>

- Audren, B., Lesgourgues, J., Benabed, K., & Prunet, S. 2013, *JCAP*, 2013, 001.
<http://stacks.iop.org/1475-7516/2013/i=02/a=001>
- Avila-Reese, V., Colín, P., Valenzuela, O., D’Onghia, E., & Firmani, C. 2001, *ApJ*, 559, 516.
<http://stacks.iop.org/0004-637X/559/i=2/a=516>
- Badertscher, A., Crivelli, P., Fetscher, W., et al. 2007, *PhRvD*, 75, 032004.
<https://link.aps.org/doi/10.1103/PhysRevD.75.032004>
- Barkana, R. 2018, *Nature*, 555, 71.
<https://www.nature.com/articles/nature25791>
- Barkana, R., Outmezguine, N. J., Redigolo, D., & Volansky, T. 2018, *PhRvD*, 98, 103005.
<https://link.aps.org/doi/10.1103/PhysRevD.98.103005>
- Batell, B., Essig, R., & Surujon, Z. 2014, *PhRvL*, 113, 171802. <https://link.aps.org/doi/10.1103/PhysRevLett.113.171802>
- Baur, J., Palanque-Desabrouille, N., Yèche, C., et al. 2017, *JCAP*, 2017, 013.
<http://stacks.iop.org/1475-7516/2017/i=12/a=013>
- Berlin, A., Hooper, D., Krnjaic, G., & McDermott, S. D. 2018, *PhRvL*, 121, 011102. <https://link.aps.org/doi/10.1103/PhysRevLett.121.011102>
- Bernardi, G., Zwart, J., Price, D., et al. 2016, *MNRAS*, 461, 2847. <http://dx.doi.org/10.1093/mnras/stw1499>
- Bertolami, M. M. M. 2014, *A&A*, 562, A123.
<https://www.aanda.org/articles/aa/abs/2014/02/aa22641-13/aa22641-13.html>
- Bezrukov, F., Chudaykin, A., & Gorbunov, D. 2018, arXiv:1809.09123. <https://arxiv.org/abs/1809.09123>
- Bird, S. A., Xue, X.-X., Liu, C., et al. 2019, *AJ*, 157, 104.
<https://iopscience.iop.org/article/10.3847/1538-3881/aafd2e/>
- Blas, D., Lesgourgues, J., & Tram, T. 2011, *JCAP*, 2011, 034. <http://stacks.iop.org/1475-7516/2011/i=07/a=034>
- Blumenthal, G. R., Faber, S. M., Primack, J. R., & Rees, M. J. 1984, *Nature*, 311, 517.
<http://dx.doi.org/10.1038/311517a0>
- Boddy, K. K., & Gluscevic, V. 2018, *PhRvD*, 98, 083510.
<https://link.aps.org/doi/10.1103/PhysRevD.98.083510>
- Boddy, K. K., Gluscevic, V., Poulin, V., et al. 2018, *PhRvD*, 98, 123506.
<https://link.aps.org/doi/10.1103/PhysRevD.98.123506>
- Bode, P., Ostriker, J. P., & Turok, N. 2001, *ApJ*, 556, 93.
<http://stacks.iop.org/0004-637X/556/i=1/a=93>
- Bose, S., Hellwing, W. A., Frenk, C. S., et al. 2017, *MNRAS*, 464, 4520.
<http://dx.doi.org/10.1093/mnras/stw2686>
- Bowman, J. D., Rogers, A. E., Monsalve, R. A., Mozdzen, T. J., & Mahesh, N. 2018, *Nature*, 555, 67.
<http://dx.doi.org/10.1038/nature25792>
- Boyarsky, A., Drewes, M., Lasserre, T., Mertens, S., & Ruchayskiy, O. 2018, *Prog. Part. and Nucl. Phys.*, doi:10.1016/j.ppnp.2018.07.004.
<https://doi.org/10.1016/j.ppnp.2018.07.004>
- Boyarsky, A., Lesgourgues, J., Ruchayskiy, O., & Viel, M. 2009a, *PhRvL*, 102, 201304. <https://link.aps.org/doi/10.1103/PhysRevLett.102.201304>
- Boyarsky, A., Ruchayskiy, O., & Iakubovskiy, D. 2009b, *JCAP*, 2009, 005. <https://iopscience.iop.org/article/10.1088/1475-7516/2009/03/005/meta>
- Bozek, B., Boylan-Kolchin, M., Horiuchi, S., et al. 2016, *MNRAS*, 459, 1489.
<http://dx.doi.org/10.1093/mnras/stw688>
- Brinckmann, T., & Lesgourgues, J. 2018, arXiv:1804.07261.
<https://arxiv.org/abs/1804.07261>
- Buen-Abad, M. A., Schmaltz, M., Lesgourgues, J., & Brinckmann, T. 2018, *JCAP*, 2018, 008.
<http://stacks.iop.org/1475-7516/2018/i=01/a=008>
- Bullock, J. S., & Boylan-Kolchin, M. 2017, *ARA&A*, 55, 343.
<https://doi.org/10.1146/annurev-astro-091916-055313>
- Cañas, B., Miranda, O., Parada, A., Tórtola, M., & Valle, J. 2016, *PLB*, 753, 191. <http://www.sciencedirect.com/science/article/pii/S0370269315009545>
- Chang, J. H., Essig, R., & McDermott, S. D. 2018, *JHEP*, 2018, 51. [https://doi.org/10.1007/JHEP09\(2018\)051](https://doi.org/10.1007/JHEP09(2018)051)
- Chen, X., Hannestad, S., & Scherrer, R. J. 2002, *PhRvD*, 65, 123515. <https://journals.aps.org/prd/abstract/10.1103/PhysRevD.65.123515>
- Chen, X., & Miralda-Escudé, J. 2004, *ApJ*, 602, 1.
<http://stacks.iop.org/0004-637X/602/i=1/a=1>
- Chianese, M., Di Bari, P., Farrag, K., & Samanta, R. 2018, arXiv:1805.11717. <https://arxiv.org/abs/1805.11717>
- Chikashige, Y., Mohapatra, R., & Peccei, R. 1981, *Physics Letters B*, 98, 265. <http://www.sciencedirect.com/science/article/pii/0370269381900113>
- Chuzhoy, L., & Kolb, E. W. 2009, *JCAP*, 2009, 014.
<http://stacks.iop.org/1475-7516/2009/i=07/a=014>
- Clark, S. J., Dutta, B., Gao, Y., Ma, Y.-Z., & Strigari, L. E. 2018, *PhRvD*, 98, 043006.
<https://link.aps.org/doi/10.1103/PhysRevD.98.043006>
- Colín, P., Avila-Reese, V., González-Samaniego, A., & Velázquez, H. 2015, *ApJ*, 803, 28.
<http://stacks.iop.org/0004-637X/803/i=1/a=28>
- Colín, P., Avila-Reese, V., & Valenzuela, O. 2000, *ApJ*, 542, 622. <http://stacks.iop.org/0004-637X/542/i=2/a=622>

- Cuoco, A., Lesgourgues, J., Mangano, G., & Pastor, S. 2005, *PhRvD*, 71, 123501.
<https://doi.org/10.1103/PhysRevD.71.123501>
- Cyburt, R. H., Fields, B. D., Olive, K. A., & Yeh, T.-H. 2016, *Rev. Mod. Phys.*, 88, 015004.
<https://link.aps.org/doi/10.1103/RevModPhys.88.015004>
- Davidson, S., Hannestad, S., & Raffelt, G. 2000, *Journal of High Energy Physics*, 2000, 003.
<http://stacks.iop.org/1126-6708/2000/i=05/a=003>
- Davis, M., Efstathiou, G., Frenk, C. S., & White, S. D. M. 1985, *ApJ*, 292, 371.
<http://adsabs.harvard.edu/abs/1985ApJ...292..371D>
- Dodelson, S. 2003, *Modern Cosmology* (New York Academic Press). <https://www.elsevier.com/books/modern-cosmology/dodelson/978-0-12-219141-1>
- Dolgov, A. D., Dubovsky, S. L., Rubtsov, G. I., & Tkachev, I. I. 2013, *PhRvD*, 88, 117701.
<https://link.aps.org/doi/10.1103/PhysRevD.88.117701>
- Dolgov, A. D., & Rudenko, A. S. 2017, *J. Exp. Theor. Phys.*, 124, 564.
<https://doi.org/10.1134/S1063776117030116>
- Dvorkin, C., Blum, K., & Kamionkowski, M. 2014, *PhRvD*, 89, 023519.
<https://link.aps.org/doi/10.1103/PhysRevD.89.023519>
- Erken, O., Sikivie, P., Tam, H., & Yang, Q. 2012, *PhRvD*, 85, 063520.
<https://doi.org/10.1103/PhysRevD.85.063520>
- Feng, C., & Holder, G. 2018, *ApJL*, 858, L17.
<http://stacks.iop.org/2041-8205/858/i=2/a=L17>
- Foot, R., Joshi, G., Lew, H., & Volkas, R. 1990, *MPL*, 95.
<https://doi.org/10.1142/S0217732390000123>
- Furlanetto, S. R., Oh, S. P., & Briggs, F. H. 2006, *PhR*, 433, 181 . <http://www.sciencedirect.com/science/article/pii/S0370157306002730>
- Gaskins, J. M. 2016, *Contemp. Phys.*, 57, 496.
<https://doi.org/10.1080/00107514.2016.1175160>
- Gluscevic, V., & Boddy, K. K. 2018, *PhRvL*, 121, 081301.
<https://link.aps.org/doi/10.1103/PhysRevLett.121.081301>
- Gninenko, S. N., Krasnikov, N. V., & Rubbia, A. 2007, *PhRvD*, 75, 075014.
<https://link.aps.org/doi/10.1103/PhysRevD.75.075014>
- Goldberg, H., & Hall, L. 1986, *PLB*, 174, 151.
[https://doi.org/10.1016/0370-2693\(86\)90731-8](https://doi.org/10.1016/0370-2693(86)90731-8)
- González-Samaniego, A., Avila-Reese, V., & Colín, P. 2016, *ApJ*, 819, 101.
<http://stacks.iop.org/0004-637X/819/i=2/a=101>
- Hills, R., Kulkarni, G., Meerburg, P. D., & Puchwein, E. 2018, *arXiv:1805.01421*.
<https://arxiv.org/abs/1805.01421>
- Hogan, C. J., & Dalcanton, J. J. 2000, *PhRvD*, 62, 063511.
<https://doi.org/10.1103/PhysRevD.62.063511>
- Holdom, B. 1986, *PLB*, 166, 196.
[https://doi.org/10.1016/0370-2693\(86\)91377-8](https://doi.org/10.1016/0370-2693(86)91377-8)
- Iršič, V., Viel, M., Haehnelt, M. G., et al. 2017, *PhRvD*, 96, 023522.
<https://link.aps.org/doi/10.1103/PhysRevD.96.023522>
- Jaeckel, J., & Ringwald, A. 2010, *Annu. Rev. Nucl. Part. Sci.*, 60, 405.
<https://doi.org/10.1146/annurev.nucl.012809.104433>
- Kadota, K., & Silk, J. 2014, *Phys. Rev. D*, 89, 103528.
<https://link.aps.org/doi/10.1103/PhysRevD.89.103528>
- Katz, A., Reece, M., & Sajjad, A. 2016, *Phys. Dark Univ.*, 12, 24 . <http://www.sciencedirect.com/science/article/pii/S2212686416000042>
- Kovetz, E. D., Poulin, V., Gluscevic, V., et al. 2018, *PhRvD*, 98, 103529.
<https://link.aps.org/doi/10.1103/PhysRevD.98.103529>
- Kovetz, E. D., Poulin, V., Gluscevic, V., et al. 2018, *arXiv:1807.11482*. <https://arxiv.org/abs/1807.11482>
- Laine, M., & Shaposhnikov, M. 2008, *JCAP*, 2008, 031.
<http://stacks.iop.org/1475-7516/2008/i=06/a=031>
- Lasserre, T. 2014, *Phys. Dark Univ.*, 4, 81.
<https://doi.org/10.1016/j.dark.2014.10.001>
- Lattanzi, M., Riemer-Sørensen, S., Tórtola, M., & Valle, J. W. F. 2013, *PhRvD*, 88, 063528.
<https://link.aps.org/doi/10.1103/PhysRevD.88.063528>
- Lesgourgues, J., Mangano, G., Miele, G., & Pastor, S. 2013, *Neutrino cosmology* (Cambridge University Press), doi:<https://doi.org/10.1017/CBO9781139012874>
- Lesgourgues, J., & Pastor, S. 2006, *PhR*, 429, 307.
<https://doi.org/10.1016/j.physrep.2006.04.001>
- Lesgourgues, J., & Tram, T. 2011, *JCAP*, 2011, 032.
<http://stacks.iop.org/1475-7516/2011/i=07/a=034>
- Liu, J., Chen, X., & Ji, X. 2017, *Nat. Phys.*, 13, 212.
<https://www.nature.com/articles/nphys4039>
- Lovell, M. R., Eke, V., Frenk, C. S., et al. 2012, *MNRAS*, 420, 2318.
<http://dx.doi.org/10.1111/j.1365-2966.2011.20200.x>
- Lovell, M. R., Bose, S., Boyarsky, A., et al. 2016, *MNRAS*, 461, 60. <http://dx.doi.org/10.1093/mnras/stw1317>
- Ma, C. P., & Bertschinger, E. 1995, *ApJ*, 455, 7.
<http://adsabs.harvard.edu/abs/1995ApJ...455....7M>
- Madau, P. 2018, *MNRAS*, 480, L43.
<http://dx.doi.org/10.1093/mnrasl/sly125>
- Madau, P., Meiksin, A., & Rees, M. J. 1997, *ApJ*, 475, 429.
<http://stacks.iop.org/0004-637X/475/i=2/a=429>
- Madsen, J. 1991, *Phys. Rev. D*, 44, 999.
<https://link.aps.org/doi/10.1103/PhysRevD.44.999>

- Marsh, D. J. 2016, *PhR*, 643, 1.
<http://dx.doi.org/10.1016/j.physrep.2016.06.005>
- McDermott, S. D., Yu, H.-B., & Zurek, K. M. 2011, *PhRvD*, 83, 063509.
<https://link.aps.org/doi/10.1103/PhysRevD.83.063509>
- Melchiorri, A., Polosa, A., & Strumia, A. 2007, *PLB*, 650, 416 . <http://www.sciencedirect.com/science/article/pii/S0370269307006375>
- Mirocha, J., & Furlanetto, S. R. 2018, arXiv:1803.03272.
<https://arxiv.org/abs/1803.03272>
- Mo, H., Van den Bosch, F., & White, S. 2010, *Galaxy formation and evolution* (Cambridge University Press).
www.cambridge.org/9780521857932
- Mohapatra, R. N., & Rothstein, I. 1990, *PLB*, 247, 593.
<http://www.sciencedirect.com/science/article/pii/S0370269390919075>
- Morales, M. F., & Wyithe, J. S. B. 2010, *ARA&A*, 48, 127.
<https://doi.org/10.1146/annurev-astro-081309-130936>
- Muñoz, J. B., Kovetz, E. D., & Ali-Haïmoud, Y. 2015, *PhRvD*, 92, 083528.
<https://link.aps.org/doi/10.1103/PhysRevD.92.083528>
- Ovanesyan, G., & Vecchi, L. 2015, *JHEP*, 2015, 128.
[https://doi.org/10.1007/JHEP07\(2015\)128](https://doi.org/10.1007/JHEP07(2015)128)
- Peccei, R. D., & Quinn, H. R. 1977, *PhRvL*, 38, 1440.
<https://link.aps.org/doi/10.1103/PhysRevLett.38.1440>
- Peebles, P. J. E. 1982, *ApJL*, 263, L1.
<http://adsabs.harvard.edu/full/1982ApJ...263L...1P>
- Pospelov, M., & ter Veldhuis, T. 2000, *PLB*, 480, 181 .
<http://www.sciencedirect.com/science/article/pii/S0370269300003580>
- Prinz, A. A., Baggs, R., Ballam, J., et al. 1998, *PhRvL*, 81, 1175.
<https://link.aps.org/doi/10.1103/PhysRevLett.81.1175>
- Pritchard, J. R., & Loeb, A. 2012, *Rep. Prog. Phys.*, 75, 086901.
<http://stacks.iop.org/0034-4885/75/i=8/a=086901>
- Raffelt, G. G. 1996, *Stars as laboratories for fundamental physics* (University of Chicago Press).
<https://www.press.uchicago.edu/ucp/books/book/chicago/S/bo3683609.html>
- Ringwald, A. 2012, *Phys. Dark Universe*, 1, 116.
<http://dx.doi.org/10.1016/j.dark.2012.10.008>
- Rodríguez-Montoya, I., Pérez-Lorenzana, A., De La Cruz-Burelo, E., Giraud-Héraud, Y., & Matos, T. 2013, *PhRvD*, 87, 025009.
<https://link.aps.org/doi/10.1103/PhysRevD.87.025009>
- Roszkowski, L., Sessolo, E. M., & Trojanowski, S. 2018, *Reports on Progress in Physics*, 81, 066201.
<https://doi.org/10.1088%2F1361-6633%2Faab913>
- Safarzadeh, M., Scannapieco, E., & Babul, A. 2018, *ApJL*, 859, L18.
<http://stacks.iop.org/2041-8205/859/i=2/a=L18>
- Sharma, P. 2018, *MNRAS*, 481, L6.
<http://dx.doi.org/10.1093/mnrasl/sly147>
- Shi, X., & Fuller, G. M. 1999, *PhRvL*, 82, 2832.
<https://link.aps.org/doi/10.1103/PhysRevLett.82.2832>
- Sigurdson, K., Doran, M., Kurylov, A., Caldwell, R. R., & Kamionkowski, M. 2004, *PhRvD*, 70, 083501.
<https://link.aps.org/doi/10.1103/PhysRevD.70.083501>
- . 2006, *PhRvD*, 73, 089903.
<https://link.aps.org/doi/10.1103/PhysRevD.73.089903>
- Sikivie, P., & Yang, Q. 2009, *PhRvL*, 103, 111301. <https://link.aps.org/doi/10.1103/PhysRevLett.103.111301>
- Singh, S., Subrahmanyam, R., Shankar, N. U., et al. 2017, *ApJL*, 845, L12.
<http://stacks.iop.org/2041-8205/845/i=2/a=L12>
- Slatyer, T. R., & Wu, C.-L. 2018, *PhRvD*, 98, 023013.
<https://link.aps.org/doi/10.1103/PhysRevD.98.023013>
- Tashiro, H., Kadota, K., & Silk, J. 2014, *PhRvD*, 90, 083522.
<https://link.aps.org/doi/10.1103/PhysRevD.90.083522>
- Tegmark, M., Eisenstein, D. J., Strauss, M. A., et al. 2006, *PhRvD*, 74, 123507.
<https://link.aps.org/doi/10.1103/PhysRevD.74.123507>
- Tremaine, S., & Gunn, J. E. 1979, *PhRvL*, 42, 407.
<https://journals.aps.org/prl/abstract/10.1103/PhysRevLett.42.407>
- Venumadhav, T., Dai, L., Kaurov, A., & Zaldarriaga, M. 2018, arXiv:1804.02406.
<https://arxiv.org/abs/1804.02406>
- Vinyoles, N., & Vogel, H. 2016, *JCAP*, 2016, 002.
<http://stacks.iop.org/1475-7516/2016/i=03/a=002>
- Voytek, T. C., Natarajan, A., García, J. M. J., Peterson, J. B., & López-Cruz, O. 2014, *ApJL*, 782, L9.
<http://stacks.iop.org/2041-8205/782/i=1/a=L9>
- Xu, W. L., Dvorkin, C., & Chael, A. 2018, *PhRvD*, 97, 103530.
<https://link.aps.org/doi/10.1103/PhysRevD.97.103530>